Resonance fluorescence spectrum of a two-level atom driven by a bichromatic field in a squeezed vacuum

Peng Zhou,[1] S. Swain,[1,2] and Z. Ficek[1,2]
[1]*Department of Applied Mathematics and Theoretical Physics, The Queen's University of Belfast, Belfast BT7 1NN, The United Kingdom*
[2]*Department of Physics, The University of Queensland, Brisbane, Queensland 4072, Australia*
(Received 4 June 1996; revised manuscript received 15 August 1996)

The steady-state resonance fluorescence spectrum of a two-level atom driven by a bichromatic field in a broadband squeezed vacuum is studied. When the carrier frequency of the squeezed vacuum is tuned to the frequency of the central spectral line, anomalous spectral features, such as hole burning and dispersive profiles, can occur at the central line. We show that these features appear for wider, and experimentally more convenient, ranges of the parameters than in the case of monochromatic excitation. The absence of a coherent spectral component at the central line makes any experimental attempt to observe these features much easier. We also discuss the general features of the spectrum. When the carrier frequency of the squeezed vacuum is tuned to the first odd or even sidebands, the spectrum is asymmetric and only the sidebands are sensitive to phase. For appropriate choices of the phase the linewidths of only the odd or even sidebands can be reduced. A dressed-state interpretation is provided. [S1050-2947(97)07302-2]

PACS number(s): 42.50.Ct, 42.50.Dv, 32.80.−t, 32.30.−r

I. INTRODUCTION

The radiative properties of atomic systems in a squeezed vacuum have been the subject of intense investigation over the past decade [1]. The most well known is the fluorescence spectrum of a two-level atom which, for a strong driving field, is a triplet with peak heights and linewidths depending on the relative phase between the driving field and the squeezed vacuum [2]. A number of other interesting modifications of the fluorescence spectrum have also been reported, such as asymmetries [3] and even suppression of the spectral lines [4]. However, the most distinctive features of the fluorescence spectrum are the hole-burning and dispersive profiles, which are qualitatively different from any features predicted before for the spectrum [5]. Asymmetries of the spectral lines can appear in the fluorescence field of a two-level atom damped by a thermal field [6], whereas the hole-burning and dispersive profiles appear only in a squeezed vacuum.

It has been shown [5] that these unusual features appear only at the central line of the incoherent component of the spectrum and occur alongside a significant reduction of the spontaneous emission from the system. They provide the most striking and unusual consequences of the interaction of atomic systems with squeezed light, and their experimental observation would be a powerful demonstration of the ability of the squeezed vacuum to modify atomic responses in a fundamental way. It has been pointed out, however, that these unusual features might be difficult to observe experimentally, as they occur at parameter values where the coherent component dominates the spectrum. Moreover, they are evident for only a highly restricted range of the parameters involved. In experiments, both the coherent and incoherent components contribute to the measured field [7]. In this paper, we show that the anomalous features also arise in the bichromatic case, but for a wider range of parameters—in particular, for a weak squeezed vacuum and large intensities of the bichromatic field—which makes the experimental observation much easier. Furthermore, there is no coherently scattered component in the bichromatic case to interfere with the observation of the incoherent spectrum [8].

We also briefly discuss the general properties of the resonance fluorescence spectrum in a bichromatic field, paying particular attention to the phase dependence of the spectrum when the squeezed vacuum is tuned respectively to the central line, the first odd, and the first even sidebands. A dressed-state interpretation of the principal features is provided.

In the absence of the squeezed vacuum, the incoherent fluorescence spectrum in an intense bichromatic field has been shown [9] to be qualitatively different from the characteristic triplet spectrum that is observed for the case of strong monochromatic excitation. Under a bichromatic excitation the spectrum consists of a series of symmetric sidebands separated by half of the frequency difference between the two components of the driving field. The separation between the sidebands is independent of the Rabi frequency of the driving field, but the number of sidebands in the spectrum increases as the Rabi frequency increases. When the components of the bichromatic field have unequal amplitudes, the spectrum is asymmetric and the central peak and even sidebands split into doublets [10]. As a result, the spectrum contains more peaks. The effect of a bichromatic laser field on the Autler-Townes spectrum has also been discussed and observed experimentally [11].

II. OPTICAL BLOCH EQUATIONS

The model is composed of a two-level atom with ground state $|g\rangle$ and excited state $|e\rangle$ and transition frequency ω_A. The atom is driven by a bichromatic laser field with frequency components $\omega_1=\omega_A-\delta_1$ and $\omega_2=\omega_A+\delta_2$, separated by $2\delta=\delta_1+\delta_2$. In general, the frequency components

can be nonsymmetrically located about the atomic frequency ω_A, with the average frequency $\omega_s=(\omega_1+\omega_2)/2$ detuned from ω_A by $\Delta=\omega_A-\omega_s$. The system (atom + bichromatic driving field) is coupled to the vacuum field, all the modes of which are assumed to be in a squeezed vacuum state.

The time evolution of the system can be described by the reduced density operator ρ, which in a frame oscillating with the frequency ω_s obeys the master equation [2,12]

$$\frac{d\rho}{dt}=-i[H,\rho]-\frac{\gamma}{2}(N+1)(\sigma_+\sigma_-\rho+\rho\sigma_+\sigma_--2\sigma_-\rho\sigma_+)$$
$$-\frac{\gamma}{2}N(\sigma_-\sigma_+\rho+\rho\sigma_-\sigma_+-2\sigma_+\rho\sigma_-)$$
$$-\gamma Me^{i\phi_s}e^{-2i(\omega_{sv}-\omega_s)t}\sigma_+\rho\sigma_+$$
$$-\gamma Me^{-i\phi_s}e^{2i(\omega_{sv}-\omega_s)t}\sigma_-\rho\sigma_-, \quad (1)$$

where $\sigma_+=|e\rangle\langle g|$ and $\sigma_-=|g\rangle\langle e|$ are the atomic raising and lowering operators, respectively, γ is the spontaneous decay rate, and

$$H=\tfrac{1}{2}\Delta\sigma_z+\Omega(\sigma_+e^{i\phi_L}\cos\delta t+\text{H.c.}), \quad (2)$$

with Ω and ϕ_L being the Rabi frequency and the phase, respectively, of the driving field. (For simplicity, we have assumed that the bichromatic field components have equal amplitudes, i.e., the field is 100% amplitude modulated.) The parameters N, M, and ϕ_s, which appear in Eq. (1), describe the squeezing of the vacuum modes. N is the squeezing photon number, M measures the strength of the two-photon correlations of the vacuum modes around the carrier frequency ω_{sv}, and ϕ_{sv} is the phase of the squeezed vacuum. We have the condition

$$M=\eta\sqrt{N(N+1)}, \quad \text{where } 0\leqslant\eta\leqslant 1 \quad (3)$$

is called the degree of correlation.

The master equation (1) leads to a closed set of three equations of motion for the expectation values of the atomic operators (the optical Bloch equations), which can be written in matrix form as

$$\frac{d}{dt}\mathbf{X}(t)=\underline{\mathcal{D}}\mathbf{X}(t)+\mathbf{L}_X. \quad (4)$$

The Bloch vector is of the form

$$\mathbf{X}(t)=\begin{bmatrix}\langle\sigma_-(t)\rangle\\ \langle\sigma_+(t)\rangle\\ \langle\sigma_z(t)\rangle\end{bmatrix},$$

the inhomogeneous term is

$$\mathbf{L}_X=\begin{bmatrix}0\\0\\-\gamma\end{bmatrix}$$

and $\underline{\mathcal{D}}$ is the 3×3 matrix

$$\underline{\mathcal{D}}=\begin{bmatrix}-(\Gamma+i\Delta) & -\xi^*e^{-2ik\delta t} & i\Omega\cos\delta t\\ -\xi e^{2ik\delta t} & -(\Gamma-i\Delta) & -i\Omega\cos\delta t\\ i2\Omega\cos\delta t & -i2\Omega\cos\delta t & -2\Gamma\end{bmatrix}, \quad (5)$$

with

$$\Gamma=\gamma(N+\tfrac{1}{2}), \quad \xi=\gamma Me^{i\Phi}, \quad \Phi=2\phi_L-\phi_{sv},$$
$$\text{and } k\delta=\omega_{sv}-\omega_s. \quad (6)$$

The parameter k indicates a detuning of the carrier frequency ω_{sv} from the central frequency ω_s: the choice $k=0$ indicates that the squeezed vacuum is centered on the central frequency, whereas $k=1$ indicates that the squeezed vacuum is centered on the first odd harmonic, and $k=2$ indicates that it is centered on the first even harmonic, of δ.

In order to solve the system of equations (4), we decompose the components $X_l(t)$ of the vector (5) into slowly varying amplitudes oscillating at the frequencies $n\delta$

$$X_l(t)=\sum_{n=-\infty}^{+\infty}X_l^{(n)}(t)e^{in\delta t}, \quad (l=1,2,3), \quad (7)$$

where $X_1(t)=\langle\sigma_-\rangle$, $X_2(t)=\langle\sigma_+\rangle$, and $X_3(t)=\langle\sigma_z\rangle$.

Substituting Eq. (7) into Eq. (4), and taking the Laplace transform, we find that the transforms $X_l^{(n)}(z)=\mathcal{L}(X_l^{(n)}(t))$, where z is the Laplace transform parameter, satisfy the vector recurrence relation

$$A_n\mathbf{X}^{(n-2k)}(z)+B_n\mathbf{X}^{(n-1)}(z)+(C_n+\mathcal{Z}_nI)\mathbf{X}^{(n)}(z)$$
$$+B_n\mathbf{X}^{(n+1)}(z)+D_n\mathbf{X}^{(n+2k)}(z)=\mathbf{X}^{(n)}(0), \quad (8)$$

where $\mathcal{Z}_n\equiv z+in\delta$, the $\mathbf{X}^{(n)}$ are column vectors

$$\mathbf{X}^{(n)}(z)=\begin{bmatrix}X_1^{(n)}(z)\\ X_2^{(n)}(z)\\ X_3^{(n)}(z)\end{bmatrix}, \quad \mathbf{X}^{(n)}(0)=\begin{bmatrix}X_1^{(n)}(0)\\ X_2^{(n)}(0)\\ X_3^{(n)}(0)-\dfrac{\gamma}{z}\delta_{n,0}\end{bmatrix}, \quad (9)$$

and A_n, B_n, C_n, and D_n are matrices

$$A_n=\begin{bmatrix}0&0&0\\ \xi&0&0\\ 0&0&0\end{bmatrix}, \quad B_n=i\tfrac{1}{2}\Omega\begin{bmatrix}0&0&-1\\ 0&0&1\\ -2&2&0\end{bmatrix},$$

$$C_n=\begin{bmatrix}\Gamma+i\Delta&0&0\\ 0&\Gamma-i\Delta&0\\ 0&0&2\Gamma\end{bmatrix}, \quad D_n=\begin{bmatrix}0&\xi^*&0\\ 0&0&0\\ 0&0&0\end{bmatrix}. \quad (10)$$

In Sec. III we will solve Eq. (10) numerically by a continued-fraction technique [13] for the steady-state values of the components $X_l^{(n)}$ and the fluorescence spectrum.

III. RESONANCE FLUORESCENCE SPECTRUM

The steady-state resonance fluorescence spectrum can be expressed in terms of the two-time correlation of the atomic operators as

$$\Lambda(\omega)=\mathrm{Re}\int_0^\infty \lim_{t\to\infty}\langle\sigma_+(t+\tau)\sigma_-(t)\rangle e^{-i(\omega-\omega_s)\tau}d\tau. \tag{11}$$

The correlation function $\lim_{t\to\infty}\langle\sigma_+(t+\tau)\sigma_-(t)\rangle$ can be calculated from the Bloch equation (4) by using the quantum regression theorem. It is not difficult to show that Eq. (1) for the two-time averages leads to the same equations as Eq. (10), but with the components $X_l^{(n)}$ replaced by $Y_l^{(n)}$ which are defined as

$$\begin{aligned} Y_1(t+\tau)&=\langle\sigma_-(t+\tau)\sigma_-(t)\rangle,\\ Y_2(t+\tau)&=\langle\sigma_+(t+\tau)\sigma_-(t)\rangle,\\ Y_3(t+\tau)&=\langle\sigma_z(t+\tau)\sigma_-(t)\rangle, \end{aligned} \tag{12}$$

and $X_l^{(n)}(0)$ replaced by

$$\begin{aligned} Y_1(0)&=0,\\ Y_2(0)&=\tfrac{1}{2}[1+\langle\sigma_z(t)\rangle],\quad Y_3(0)=-\langle\sigma_-(t)\rangle. \end{aligned} \tag{13}$$

The steady-state resonance fluorescence spectrum can then be found from

$$\Lambda(\omega)=\mathrm{Re}[Y_2^{(0)}(z)]_{z=i(\omega-\omega_s)}. \tag{14}$$

In the following, we plot the fluorescence spectrum for a strong driving field ($\Omega\gg\gamma$) with the central frequency resonant with the atomic frequency, i.e., $\Delta=0$, and three different values of k: $k=0$, 1, and 2.

A. The case of $k=0$

First, we consider the case when the carrier frequency of the squeezed vacuum is tuned to the central spectral frequency, $\omega_{sv}=\omega$ ($k=0$). Figure 1 shows the fluorescence spectrum of a two-level atom driven by a bichromatic laser field with $\Omega=5\gamma$, $\delta=10\gamma$, in a squeezed vacuum with $N=0.1$, and with the two phases $\Phi=0$ and π. We see that the general spectral structures in the presence of a squeezed vacuum are qualitatively similar to those in the standard vacuum with the central component located at ω_s and the sidebands located at $\omega_s\pm n\delta$, where n is an integer. However, the central component is dramatically modified by the squeezed vacuum. For $\Phi=0$ the central component is greatly suppressed, whereas for $\Phi=\pi$ it dominates the spectrum and is very narrow. On the other hand, the sidebands vary slowly with the phase and exhibit a slight broadening when Φ increases from 0 to π.

Although not very evident in Fig. 1, the reduction of the amplitude of the central line for $\Phi=0$ leads to the appearance of shallow dip at line center. (The dip *is* obvious in Figs. 4–6.) The observation of this dip would be a matter of some importance, since it only arises in the presence of the squeezed vacuum. As we know, such dips can also appear in

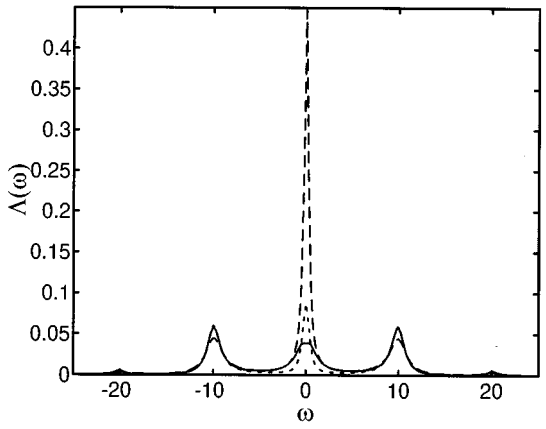

FIG. 1. The resonance fluorescence spectrum of a two-level atom driven by a bichromatic field in a squeezed vacuum whose carrier frequency is tuned to the central spectral frequency, as a function of ω, with the parameters: $\Omega=5\gamma, \delta=10\gamma$, and $N=0.1$. The solid curves are for $\Phi=0$, the dash lines for $\Phi=\pi$, and the dotted lines give the corresponding spectrum in the absence of the squeezed vacuum. In all our figures, frequencies are measured in units of γ.

a two-level system driven by a monochromatic laser field [5]. However, there are marked differences between the monochromatic and bichromatic cases. These differences will become apparent as we present more plots, but we summarize the major points here. In the former case, the dip becomes more pronounced as the squeezed photon number N increases, whereas in the bichromatic case, we find that the dip is clearly present for very small values of N, and in fact is most pronounced for small N. (It actually disappears for large N values, unlike the monochromatic case.) For the monochromatic case, the dip occurs for small driving intensities, $\Omega\simeq\gamma$. This has the disadvantage that the coherent scattering present in this case is strong, and may obscure the observation of the dip in the incoherent part of the spectrum. In the case of a bichromatic driving field the dip may occur for large intensities of the driving field, and there is no coherent scattering. We also have an extra parameter, δ, in the bichromatic case, and we may choose this quantity so as to maximize the effects we are investigating. Finally, in the monochromatic case, the dip is very sensitive to the value of η—it has to be very close to one—whereas in the bichromatic case we can find parameter values such that the dip is relatively insensitive to the value of η. All these factors contribute to making the observation of the dip much easier in the bichromatic case than the monochromatic case.

In the monochromatic case, the anomalous features occurred when the incoherent intensity at line center, $\Lambda(0)$, was a minimum [5]. To investigate whether this property also holds for bichromatic excitation, we plot the value of the resonance fluorescence at the line center as a function of the Rabi frequency Ω for various small values of N in Fig. 2, with $\delta=10\gamma$ and $\Phi=0$. In the absence of the squeezing: $N=0$, shown in the frame Fig. 2(a), the quantity $\Lambda(0)$ increases from zero monotonically then oscillates with Ω. However, if a squeezed vacuum is applied, as shown in the remaining frames, the quantity $\Lambda(0)$ is non-zero at $\Omega=0$, decreases to a minimum then increases as Ω increases, and finally oscillates with increasing Rabi frequency. The existence of the first minimum is due to the presence of the

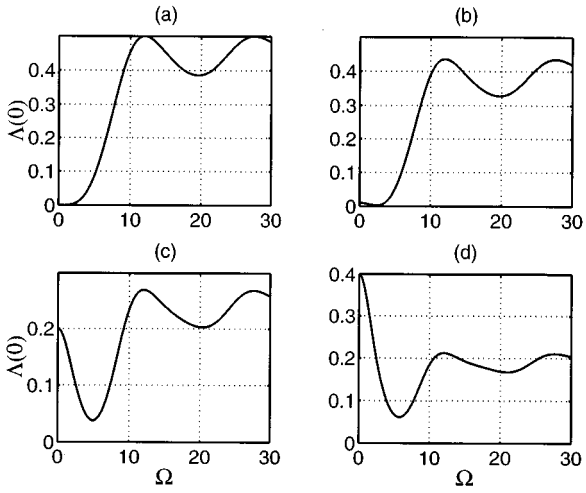

FIG. 2. The resonance fluorescence at line center, $\omega=\omega_s$, as a function of Ω, for $\delta=10$, $\Phi=0$, and (a) $N=0$, (b) $N=0.005$, (c) $N=0.1$, (d) $N=0.2$.

squeezed vacuum. Hereafter, we shall call it the *squeezing-induced minimum*. It is at the squeezing-induced minimum that we would expect to see distinctive spectral features in the resonance fluorescence spectrum, as found for the system driven by a monochromatic laser. The higher-order minima do not give rise to anomalous features.

In the bichromatic case, we have the extra parameter δ. Figure 3 presents a three-dimensional plot of $\Lambda(0)$ against δ and Ω, and shows that the value of Ω at which the first minimum occurs increases steadily with δ. Note however that the absolute value of the first minima remains small as δ increases, showing that the anomalous features should persist for large as well as small δ values.

Figure 4 shows the fluorescence spectrum in the vicinity of the squeezing-induced minimum, with the parameters: $\delta=10\gamma, \Phi=0$, and $N=0.005$, corresponding to frame (b) of Fig. 2. A hole with subnatural linewidth is clearly exhibited at line center. By numerical calculation, we find that the hole burning can only occur when the value of the squeezing-induced minimum is very small (close to zero). It is also essential for the squeezed vacuum to be weak. For stronger squeezed vacua, for example, $N=0.2$ (the graph is not shown here), no dip occurs at all, although there is a minimum induced by the squeezed vacuum at line center, as shown in Fig. 2(d).

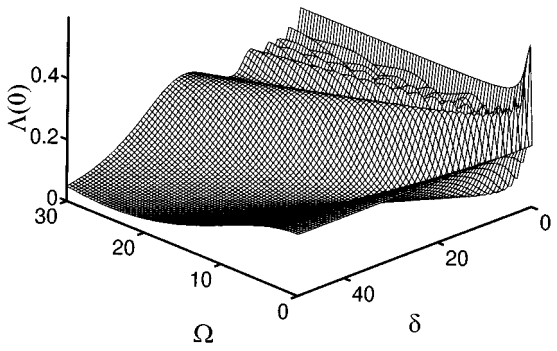

FIG. 3. The resonance fluorescence at line center, $\omega=\omega_s$, as a function of Ω and δ for $\Phi=0$ and $N=0.1$.

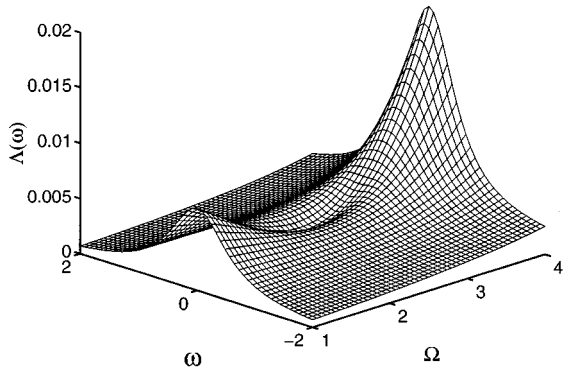

FIG. 4. The three-dimensional resonance fluorescence spectrum in the vicinity of the squeezing-induced minimum, for $\delta=10\gamma$, $\Phi=0$, and $N=0.005$.

In Fig. 5 we assume a large Rabi frequency for the driving field ($\Omega=10\gamma$) and plot the spectrum for different values of δ. In this case also the dip is pronounced, the greatest effect occurring at quite a large value of the frequency difference δ. In Fig. 6 we show the dips of Figs. 4 and 5 in a two-dimensional plot, for greater clarity.

Another factor which makes observation of the anomalous features difficult in the monochromatic case is the rapid disappearance of the anomalous features as the degree of correlation η decreases from its ideal value of unity. The disappearance is particularly rapid for the larger values of N. In Fig. 7 we plot the spectrum $\Lambda(\omega)$ for $N=0.005$, $\Phi=0$, and $\Omega=2.4\gamma$ for the values $\eta=1,0.9$ and 0.8. It can be seen that the anomalous features disappear rather slowly with η in the bichromatic case.

Now we consider the effect of choosing phase values other than $\Phi=0$. We find that the anomalous features disappear as Φ increases much more rapidly in the bichromatic case than in the monochromatic case. In fact, we need to restrict our attention to values $|\Phi|\leq\pi/8$ in the former situation, whereas in the monochromatic case, anomalous features occurred for $\Phi>\pi/2$. Figure 8 shows the fluorescence spectrum for the same parameters as in Fig. 5, but with $\Phi=\pi/10$. In this case there is a dispersive profile at line center. As pointed out in Ref. [5] , the dispersive profile in the fluorescence is another distinctive feature, which appears

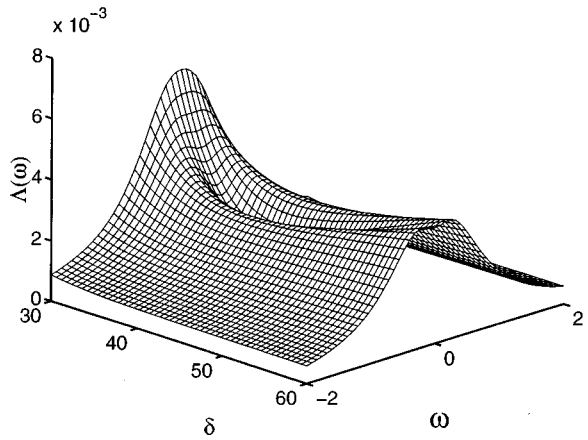

FIG. 5. Same as Fig. 3, but with $\Omega=10\gamma$ and δ varying.

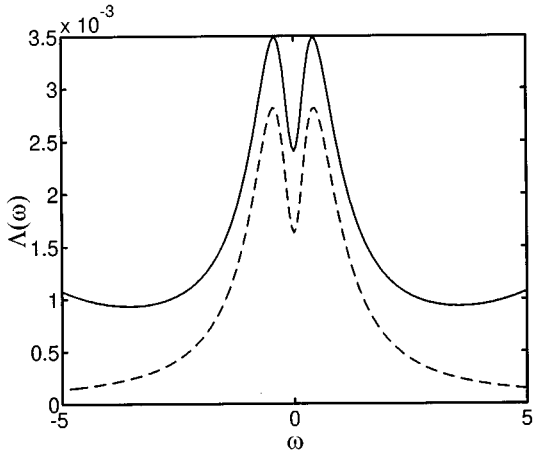

FIG. 6. The resonance fluorescence spectrum near the squeezing-induced minimum for $\Phi=0$, $N=0.005$ and (a) $\Omega=2.5\gamma$, $\delta=10\gamma$, (solid line) and (b) $\Omega=10\gamma$, $\delta=40\gamma$ (dashed line).

only in the squeezed vacuum. Again, in the bichromatic field the dispersive profiles appear for a weak squeezed vacuum and large Rabi frequencies of the driving field.

We have emphasized that the anomalous spectral features in the incoherent spectrum would be very difficult to observe in the monochromatic case, since for the low driving intensities at which they arise, coherent fluorescence at line center dominates. However, in the bichromatic case, the coherent fluorescence component is given by [8]

$$\Lambda_{coh}(\omega)=\mathrm{Re}\int_0^\infty \lim_{t\to\infty}\langle\sigma_+(t+\tau)\rangle\langle\sigma_-(t)\rangle e^{-i(\omega-\omega_s)\tau}d\tau$$

$$=\sum_{n=-\infty}^{+\infty}|X_1^{(n)}|^2\delta(\omega-\omega_s+n\delta), \tag{15}$$

and occurs at frequencies $\omega=\omega_s\pm n\delta$, where n is an odd

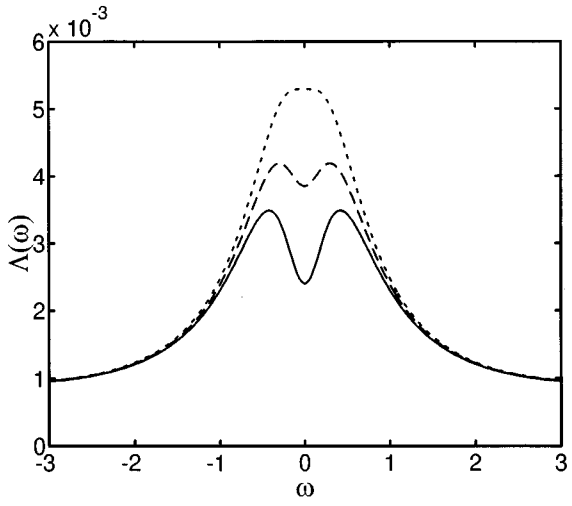

FIG. 7. The resonance fluorescence spectrum with the parameters: $\Omega=2.5\gamma$, $\Phi=0$, $\delta=10\gamma$, and $N=0.005$, for different values of the degree of correlation: (a) $\eta=1$ (solid line), (b) $\eta=0.9$ (dashed line), and (c) $\eta=0.8$ (dotted line).

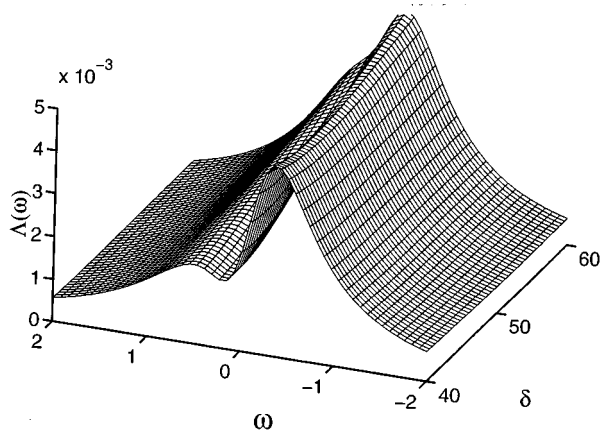

FIG. 8. Same as Fig. 5, but for $\Phi=\pi/10$.

number. Therefore, there is no coherent component at line center to interfere with the experimental observation of anomalous spectra.

B. The case of $k\neq 0$

The recurrence relation (10) permits us to calculate the fluorescence spectrum for a squeezed vacuum tuned to one of the spectral sidebands. The case of $k=1$ corresponds to the squeezed vacuum tuned to the first odd sideband at $\omega-\omega_s=\delta$. Figure 9 shows the spectrum for $k=1$, $\delta=10\gamma$, $\Omega=15\gamma$ and different phases. The spectrum is qualitatively unchanged, but in contrast to the case $k=0$, the central component of the spectrum exhibits a small variation with the phase. However, the odd sidebands broaden whereas the even sidebands narrow as the phase varies from 0 to π. Moreover, for the latter value of the phase, the amplitudes of the odd sidebands are asymmetric around $\omega-\omega_s=0$.

The phase properties of the spectral sidebands are quite different when the squeezed vacuum is tuned to the first even sideband. This is shown in Fig. 10, where we plot the spectrum for the same parameters as in Fig. 9, but with $k=2$. In this case the squeezed vacuum is tuned to the even sideband

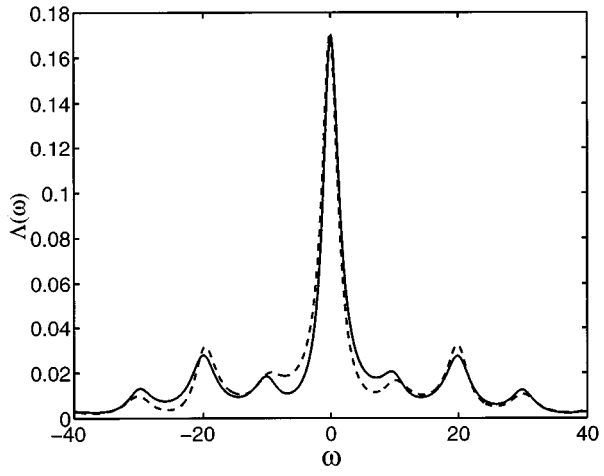

FIG. 9. The resonance fluorescence spectrum for the squeezed vacuum tuned to the first odd sideband, with $k=1$, $\delta=10\gamma$, $\Omega=15\gamma$, $N=1$, and different phases. The solid curves are for $\Phi=0$, and the dashed lines for $\Phi=\pi$.

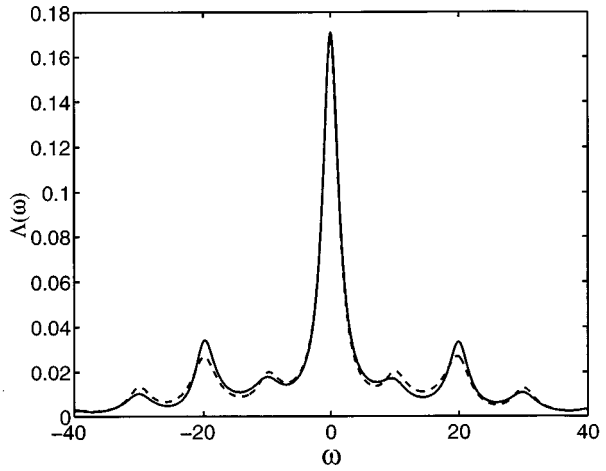

FIG. 10. Same as Fig. 9, but for the squeezed vacuum tuned to the first even sideband, i.e., $k=2$.

at $\omega-\omega_s=2\delta$. Again, the spectrum is qualitatively unchanged, but now the odd sidebands narrow and the even sidebands broaden when the phase varies from 0 to π.

IV. DRESSED-STATE INTERPRETATION

We may gain a qualitative understanding of the phase dependence of the width and height of the central peak by considering the spectra for the special cases $\Delta=0$, $k=0$, and $\Phi=0,\pi$. It is convenient to rewrite the two-time correlation function $\langle\sigma_+(t+\tau)\sigma_-(t)\rangle$, and the Bloch equation in terms of the in-phase and out-phase quadratures of the atomic dipole, $\sigma_x=(\sigma_-+\sigma_+)$ and $\sigma_y=i(\sigma_--\sigma_+)$:

$$\langle\sigma_+(t+\tau)\sigma_-(t)\rangle=\langle\sigma_x(t+\tau)\sigma_x(t)\rangle+\langle\sigma_y(t+\tau)\sigma_y(t)\rangle -i\langle\sigma_x(t+\tau)\sigma_y(t)\rangle+i\langle\sigma_y(t+\tau)\sigma_x(t)\rangle \tag{16}$$

and

$$\langle\dot{\sigma}_x\rangle=-\gamma_x\langle\sigma_x\rangle,\quad \langle\dot{\sigma}_y\rangle=-\gamma_y\langle\sigma_y\rangle-2\Omega\cos\delta t\langle\sigma_z\rangle,$$
$$\langle\dot{\sigma}_z\rangle=-\gamma_z\langle\sigma_z\rangle+2\Omega\cos\delta t\langle\sigma_y\rangle-\gamma, \tag{17}$$

with

$$\gamma_x=\Gamma+\gamma M\cos\Phi\quad(\Phi=0,\pi),$$
$$\gamma_y=\Gamma-\gamma M\cos\Phi\quad(\Phi=0,\pi),$$
$$\gamma_z=\gamma_x+\gamma_y. \tag{18}$$

It is evident that the motion of the x-polarized quadrature $\langle\sigma_x\rangle$ is decoupled from that of the y-polarized quadrature $\langle\sigma_y\rangle$ and the inversion $\langle\sigma_z\rangle$ which are entangled by the bichromatic field. As a consequence, the atomic correlation function $[\langle\sigma_x(t+\tau)\sigma_x(t)\rangle-i\langle\sigma_x(t+\tau)\sigma_y(t)\rangle]$, which by the quantum regression theorem follows the free decay of the x-polarized quadrature at rate γ_x, makes a contribution only to the central peak of the resonance fluorescence spectrum. However, the correlation function $[\langle\sigma_y(t+\tau)\sigma_y(t)\rangle+i\langle\sigma_y(t+\tau)\sigma_x(t)\rangle]$, which is determined by the remaining coupled Bloch equations, also makes a contribution to the central component as well as to the sidebands. Numerical calculations show that the contribution of this correlation function to the central component is zero for $N=0$, the standard vacuum, and is negative for a weak squeezed vacuum ($N\ll1$), resulting in a dip at line center. However, for almost all parameter values, the magnitude of the negative component is very small compared to the positive contribution, and the central component is well approximated by

$$\Lambda_{center}(\omega)=\frac{2\gamma_x I_{tot}^{ss}}{\gamma_x^2+(\omega-\omega_A)^2}, \tag{19}$$

where $I_{tot}^{ss}=(1+X_3^{(0)})/2$ is the steady-state fluorescence intensity.

An exception occurs near the squeezing-induced minimum, when the overall magnitude of the central line is greatly reduced, enabling the negative dip to become significant and giving rise to the anomalous features described earlier (Figs. 4–8). The negative contribution from the final pair of the Eqs. (17) actually has two components: one, a broad negative peak, acts to reduce the overall intensity of the fluorescence near line center, as can be seen in Fig. 2, while the other, a sharp negative peak, acts to produce the dip at line center.

Away from the squeezing-induced minimum, the central spectral component clearly has a linewidth $2\gamma_x=2(\Gamma+\gamma M\cos\Phi)$ $(\Phi=0,\pi)$, which is dependent on the squeezed phase. The linewidth for $\Phi=0$ is much greater than that for $\Phi=\pi$ when the squeezed photon number $N\gg1$. The phase sensitivity of the central spectral linewidth is similar to that of the case of a monochromatic field excitation [2].

On the other hand, the height of the central peak,

$$H_{center}=\frac{2I_{tot}^{ss}}{\gamma_x}, \tag{20}$$

is strongly sensitive to the squeezed photon number N and phase Φ, and is proportional to the steady-state fluorescence intensity I_{tot}^{ss} that oscillates with the Rabi frequency Ω [10]. In a standard vacuum, the height is extremely small for very low Rabi frequencies. However, in the presence of a squeezed vacuum, the height may be larger, even for a very small value of Ω, due to the saturating effect of the squeezed vacuum on the total fluorescence intensity I_{tot}^{ss}. In general, for fixed Ω and N, the height H_{center} for $\Phi=\pi$ is higher than that for $\Phi=0$. However, for a given Rabi frequency Ω, the height decreases as the photon number increases for $\Phi=0$. All these features result from the phase-sensitive decays of the atomic dipole induced by the squeezed vacuum.

The spectral features are a direct signature of the energy structures of the atom-field interaction. In the system of a two-level atom with the ground and excited states, $|g\rangle$ and $|e\rangle$, interacting with a bichromatic laser at frequencies $\omega_A\pm\delta$ (assuming $\omega_A\gg\delta$), for a total excitation quantum number $\mathcal{N}=n_1+n_2+n_a$ (where n_1,n_2 are the photon numbers of the two frequency components of the bichromatic field, and $n_a=(0,1)$ represents the atom in the ground or excited states, respectively), the product states of the bare atom and field, $|n,\mathcal{N}-n,g\rangle$, $(n=0,1,2,\ldots,\mathcal{N})$ and $|n,\mathcal{N}-n-1,e\rangle$, $(n=0,1,2,\ldots,\mathcal{N}-1)$ are all nearly degenerate and are strongly mixed by the atom-field interac-

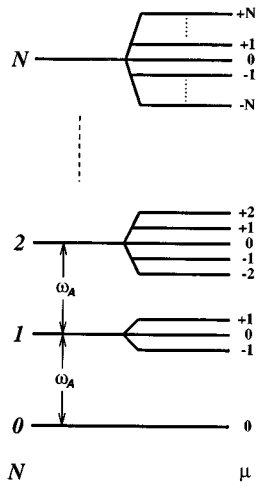

FIG. 11. The energy level structure of the dressed-atom states.

tion: they form the $\mathcal{N}$th state manifold which has degeneracy $2\mathcal{N}+1$. For example, in the ground-state manifold of the atom-field interaction, $\mathcal{N}=0$, the only state is $|0,0,g\rangle$, where the atom is in its ground state with no photons in either mode, while the first excited-state manifold, $\mathcal{N}=1$, consists of the atom in the excited state with no photons in either field, $|0,0,e\rangle$, or in the ground state with 1 photon in either mode, $|1,0,g\rangle$ and $|0,1,g\rangle$.

It is well known that in the dressed-atom picture the $\mathcal{N}$th manifold is composed of $2\mathcal{N}+1$ equally spaced dressed states with separation δ, which are linear combinations of the bare states [9,10,16,14]. See Fig. 11, where the energy level structure of the dressed atom is exhibited.

The resonance fluorescence is described by a cascade of population down the quantum ladder of the dressed state manifold. The nature of the dipole coupling allows transitions only from the manifold $\mathcal{N}$ to the manifold $\mathcal{N}-1$, with no spontaneous transitions within each sublevel [15].

At very small Rabi frequencies Ω, the atom-bichromatic field interaction can only populate the lowest two dressed-state manifolds, $\mathcal{N}=0$ and 1. Therefore, only three spontaneous emissions are probable, from the $\mathcal{N}=1$ manifold with three components to the $\mathcal{N}=0$ manifold consisting of a single dressed level. Accordingly, the resonance fluorescence spectrum consists of three components located at frequencies $\omega_A, \omega_A \pm \delta$. As the Rabi frequency increases, the interaction of the atom with the field is likely to populate higher dressed-state manifolds, leading for example to transitions from the $\mathcal{N}=2$ manifold consisting of five dressed states to the $\mathcal{N}=1$ manifold, then to the ground state, so that the number of lines present in the resonance fluorescence spectrum increases. The positions of the spectral lines are determined by the splitting of the dressed states, δ, which is independent on the Rabi frequency. However, the heights of the spectra are proportional to the populations of the corresponding dressed states. It is well known that the dressed-state populations in such a system are associated with Bessel functions of argument δ/Ω [9,10,16,17], which oscillate. For certain values of Ω, the Bessel functions may be zero, resulting in the vanishing of populations and the resulting disappearance of the corresponding spectral lines. Because of the symmetric distribution of the dressed-state populations about the central dressed state in each manifold [10,17], the resonance fluorescence spectrum is symmetric about the atomic frequency ω_A.

If the bichromatic field components have unequal amplitudes, or if the center frequency is detuned from ω_A ($\Delta \neq 0$), the symmetric distribution of populations is destroyed and dressed state levels are shifted strongly depending on the ratio of the amplitudes and Δ. As a result, the spectra are asymmetric [10]. For certain situations, some of the dressed states may be trapped. Accordingly, the spontaneous emission from these trapped levels will be quenched and the corresponding spectral lines will disappear [4].

V. SUMMARY

We have calculated the resonance fluorescence spectrum of a two-level atom driven by a bichromatic laser in a frequency-tunable squeezed vacuum by using continued-fraction methods. We have evaluated the spectrum numerically in the three cases where the carrier frequency of the squeezed vacuum is tuned close to the central spectral line, and the first-odd and first-even sideband, respectively. Apart from the anomalous feature which may arise at line center, the general spectral structures are qualitatively similar to those in the normal vacuum: the sidebands are placed at $\omega_s \pm n\delta$ where n is an integer, and the number of the sidebands increases as the driving intensity increases. However, they are, in general, phase sensitive. We have indicated how the dressed-state picture may be used to understand these features.

We have been particularly interested in the occurrence of the anomalous spectral features at the central line, such as hole-burning and dispersive profiles. We have shown that in the case of the squeezed vacuum coupled to the central component these features can occur for a wide range of the parameters—in particular, for a weak squeezed vacuum and high intensities of the bichromatic laser field. The absence of coherent scattering at line center provides the major advantage of bichromatic excitation for observing the anomalous spectral features as compared with the monochromatic case. A number of other features, such as the relatively slow decline of the anomalous features with decreasing η, combine to make the bichromatic situation more favorable to experiment.

In the case of the squeezed vacuum coupled to the first-odd or first-even sidebands, the spectrum is asymmetric and only the sidebands are sensitive to the phase.

We note that Polzik, Carri, and Kimble [18] have recently developed a frequency-tunable source of squeezed light suitable for spectroscopic applications over a broad range. It has been successfully applied to exploring the modification of atomic radiative properties in the presence of squeezed light in a recent landmark experiment [19], where they observed that the two-photon excitation of atoms by a squeezed vacuum possesses a component linear in the squeezed photon number, as predicted theoretically [20]. This experimental progress could make it possible to observe the anomalous features in the resonance fluorescence spectrum in the near future.

ACKNOWLEDGMENTS

This work is supported by the United Kingdom EPSRC, by the EC, and by a NATO collaborative research grant. We would like to thank Dr. B. J. Dalton and Dr. T. A. B. Kennedy for helpful conversations. P.Z. wishes to thank Queen's University for financial support. S.S. would like to thank the University of Queensland for financial support.

[1] See, for example, A. S. Parkins, in *Modern Nonlinear Optics, Part 2*, edited by M. Evans and S. Kielich (Wiley, New York, 1993), p. 607.

[2] H. J. Carmichael, A. S. Lane, and D. F. Walls, Phys. Rev. Lett. **58**, 2539 (1987); J. Mod. Opt. **34**, 821 (1987).

[3] S. Smart and S. Swain, Quantum Opt. **5**, 75 (1993).

[4] J. M. Courty and S. Reynaud, Europhys. Lett. **10**, 237 (1989); C. Cabrillo, W. S. Smyth, S. Swain, and P. Zhou, Opt. Commun. **114** , 344 (1995).

[5] S. Smart and S. Swain, Phys. Rev. A **48**, R50 (1993); S. Swain, Phys. Rev. Lett. **73**, 1493 (1994); S. Swain and P. Zhou, Phys. Rev. A **52**, 4845 (1995).

[6] G. P. Hildred, S. S. Hassan, R. R. Puri, and R. K. Bullough, J. Phys. B **16**, 1703 (1983); S. S. Hassan, G. P. Hildred and R. K. Bullough, *ibid.* **21**, 981 (1983).

[7] F. Y. Wu, R. E. Grove, and S. Ezekiel, Phys. Rev. Lett. **35** , 1426 (1977); J. D. Cresser, J. Hager, G. Leuchs, M. Rateike, and H. Walther, in *Dissipative System in Quantum Optics*, edited by R. Bonifacio (Springer-Verlag, Berlin, 1982), p. 21.

[8] B. Blind, P. R. Fontana, and P. Thomann, J. Phys. B **13**, 2717 (1980); G. S. Agarwal, Y. Zhu, D. J. Gauthier, and T. W. Mosserg, J. Opt. Soc. Am. B **8**, 1163 (1991).

[9] Y. Zhu, Q. Wu, A. Lezama, D. J. Gauthier, and T. W. Mossberg, Phys. Rev. A **41**, R6574 (1990); H. S. Freedhoff and Z. Chen, *ibid.* **41**, 6013 (1990); S. P. Tewari and M. K. Kumari, *ibid.* **41**, R5273 (1990).

[10] Z. Ficek and H. S. Freedhoff, Phys. Rev. A **48**, 3092 (1993); Phys. Rev. A **53**, 4275 (1996).

[11] M. F. Van Leeuwen, S. Papademetriou, and C. R. Stroud, Jr., Phys. Rev. A **53**, 990 (1996); S. Papademetriou, M. F. Van Leeuwen, and C. R. Stroud, Jr., *ibid.* **53**, 997 (1996).

[12] C. W. Gardiner, Phys. Rev. Lett. **56**, 1917 (1986).

[13] H. Risken, in *The Fokker-Planck Equation* (Springer-Verlag, Berlin, 1984), Chap. 9; S. Swain, Adv. At. Mol. Phys. **22**, 387 (1986).

[14] P. M. Alsing, D. A. Cardimona, and H. J. Carmichael, Phys. Rev. A **45**, 1793 (1992); G. S. Agarwal, W. Lange, and H. Walther, *ibid.* **51**, 721 (1995).

[15] M. A. Newblod and G. J. Salamo, Phys. Rev. A **22**, 2098 (1980); S. P. Tewari and M. K. Kumari, *ibid.* **41**, R5273 (1990).

[16] G. S. Agarwal, Y. Zhu, D. J. Gauthier, and T. W. Mosserg, J. Opt. Soc. Am. B **8**, 1163 (1991).

[17] H. S. Freedhoff and Z. Chen, Phys. Rev. A **41**, 6013 (1990); **46**, 7328(E) (1992).

[18] E. S. Polzik, J. Carri, and H. J. Kimble, Phys. Rev. Lett. **68**, 3020 (1992).

[19] N. Ph. Georgiades, E. S. Polzik, K. Edamtsu, H. J. Kimble, and A. S. Parkins, Phys. Rev. Lett. **75**, 3426 (1995).

[20] J. Gea-Banacloche, Phys. Rev. Lett. **62**, 1603 (1989); J. Javanainen and P. L. Gould, Phys. Rev. A **41**, 5088 (1990); Z. Ficek and P. D. Drummond, Phys. Rev. A **44**, 6247 (1991); **44**, 6258 (1991); C. W. Gardiner and A. S. Parkins, *ibid.* **50**, 1792 (1994); P. Zhou and S. Swain, *ibid.* **54**, 4275 (1996).